

# Synchronization of pitch and plunge motions during intermittency route to aeroelastic flutter

Cite as: Chaos **29**, 043129 (2019); <https://doi.org/10.1063/1.5084719>

Submitted: 06 December 2018 . Accepted: 05 April 2019 . Published Online: 29 April 2019

Ashwad Raaj, J. Venkatramani, and Sirshendu Mondal 



View Online



Export Citation



CrossMark

## ARTICLES YOU MAY BE INTERESTED IN

[Bursting and mixed mode oscillations during the transition to limit cycle oscillations in a matrix burner](#)

Chaos: An Interdisciplinary Journal of Nonlinear Science **29**, 043117 (2019); <https://doi.org/10.1063/1.5095401>

[Sparse learning of partial differential equations with structured dictionary matrix](#)

Chaos: An Interdisciplinary Journal of Nonlinear Science **29**, 043130 (2019); <https://doi.org/10.1063/1.5054708>

[Interplay between random fluctuations and rate dependent phenomena at slow passage to limit-cycle oscillations in a bistable thermoacoustic system](#)

Chaos: An Interdisciplinary Journal of Nonlinear Science **29**, 031102 (2019); <https://doi.org/10.1063/1.5088943>

AIP Author Services  
English Language Editing



# Synchronization of pitch and plunge motions during intermittency route to aeroelastic flutter

Cite as: Chaos 29, 043129 (2019); doi: 10.1063/1.5084719

Submitted: 6 December 2018 · Accepted: 5 April 2019 ·

Published Online: 29 April 2019




View Online



Export Citation



CrossMark

Ashwad Raaj,<sup>1</sup> J. Venkatramani,<sup>1</sup> and Sirshendu Mondal<sup>2,a)</sup> 

## AFFILIATIONS

<sup>1</sup>Department of Mechanical Engineering, Shiv Nadar University, Greater Noida 201314, India

<sup>2</sup>Department of Mechanical Engineering, National Institute of Technology, Durgapur 713209, India

<sup>a)</sup>Electronic mail: [sirshendumondal13@gmail.com](mailto:sirshendumondal13@gmail.com)

## ABSTRACT

Interaction of fluid forces with flexible structures is often prone to dynamical instabilities, such as aeroelastic flutter. The onset of this instability is marked by sustained large amplitude oscillations and is detrimental to the structure's integrity. Therefore, investigating the possible physical mechanisms behind the onset of flutter instability has attracted considerable attention within the aeroelastic community. Recent studies have shown that in the presence of oncoming fluctuating flows, the onset of flutter instability is presaged by an intermediate regime of oscillations called intermittency. Further, based on the intensity of flow fluctuations and the relative time scales present in the flow, qualitatively different types of intermittency at different flow regimes have been reported hitherto. However, the coupled interaction between the pitch (torsion) and plunge (bending) modes during the transition to aeroelastic flutter has not been explored. With this, we demonstrate with a mathematical model that the onset of flutter instability under randomly fluctuating flows occurs via a mutual phase synchronization between the pitch and the plunge modes. We show that at very low values of mean flow speeds, the response is by and large noisy and, consequently, a phase asynchrony between the modes is present. Interestingly, during the regime of intermittency, we observe the coexistence of patches of synchronized periodic bursts interspersed amidst a state of desynchrony between the pitch and the plunge modes. On the other hand, at the onset of flutter, we observe a complete phase synchronization between the pitch and plunge modes. This study concludes by utilizing phase locking value as a quantitative measure to demarcate different states of synchronization in the aeroelastic response.

Published under license by AIP Publishing. <https://doi.org/10.1063/1.5084719>

Elastic structures, such as aircraft wings, when subjected to fluid loads lead to the formation of a mutual coupling between the flow and the structure. At a critical value of the flow speed, there is a sustained transfer of energy from the flow to the structure, resulting in a dynamic instability called aeroelastic flutter. This instability is self-feeding in nature and typically leads to structural failure. Consequently, the aeroelastic community hitherto has devoted substantial attention toward examining the mechanisms that could possibly lead to flutter instability. However, the presence of nonlinearities and input fluctuating flows pose a challenge in discerning the underlying mechanisms. This study devotes its attention to this concern. Accordingly, a three-dimensional wing is considered as a two degrees of freedom (2-DOF) airfoil in the form of pitch (torsion) and plunge (bending) modes. The input flow is modeled as randomly varying with time. By obtaining the time histories of the aeroelastic responses, we address the tran-

sition to aeroelastic flutter from the parlance of synchronization theory. Typically, a key step in synchronization studies involves investigating a possible locking of phase/frequency values of the output time responses. To that end, a considerable understanding of the synchronization in chaotic and periodic oscillations can be found in the literature. However, in scenarios involving intermittent responses in the preflutter regime, the use of synchronization framework demands further investigations. Here, we investigate the coupled interaction between the pitch and the plunge modes as the system transitions to flutter by performing numerical experiments. To do the same, the relative phase between the pitch and plunge oscillations is sought by invoking quantitative measures such as phase locking value (PLV). It is revealed that the transition to flutter is through a regime of intermittently phase synchronized pitch and plunge modes, and, at the onset of flutter, complete synchronization between the modes is observed.

## I. INTRODUCTION

Aeroelastic flutter is a manifestation of dynamic instability involving a continuous transfer of energy from the flow to the structure. This instability is characterized by the onset of limit cycle oscillations (LCOs) in the aeroelastic responses.<sup>1</sup> Indeed, sustained large amplitude LCOs experienced by the structure can lead to abrupt failure due to overloading (or) lead to gradual failure due to the development of fatigue cracks. Consequently, ensuring that operating conditions do not transgress into regimes of aeroelastic flutter is of key importance. Preventing the onset of flutter is possible only when the flutter boundaries are accurately obtained—which in turn depends on the underlying description of the physical mechanism that leads to this instability. Therefore, the physical insights behind the onset of flutter have been extensively explored through both wind tunnel experiments and numerical simulations.

Traditionally, in a two degrees of freedom (2-DOF) airfoil with the pitch (torsion) and plunge (bending) modes, the onset of flutter is explained by the coalescence of the modal frequencies.<sup>2</sup> Here, the modal frequencies refer to the frequencies of the pitch and the plunge modes. This form of flutter is known as classical flutter or binary flutter. Studies involving linear aeroelastic models were found to be inaccurate in capturing the dynamics due to abrupt transitions to flutter<sup>3</sup> and manifestation of LCOs in the postflutter regime.<sup>4–6</sup> Consequently, nonlinearities in the structure or the aerodynamics of the flow were modeled to account for the same. Shocks in transonic and supersonic flow regimes and flow separation in the presence of large angles of attack are examples of aerodynamical nonlinearities.<sup>6</sup>

The inclusion of nonlinearities in the aeroelastic system leads to qualitative changes in the topology of its state space. Consequently, one encounters a variety of bifurcations and in turn a variety of nonlinear dynamical responses. For example, the inclusion of cubic nonlinearity in stiffness is reported to give rise to Hopf bifurcation.<sup>6</sup> At the flutter speed, the response dynamics transforms into sustained LCOs and for flow speeds lower than the flutter speed, a decaying signature in the response is observed. Introducing cubic nonlinearities in both pitch and plunge degrees of freedom (coupled cubic nonlinearities) can give rise to phenomenologically rich nonlinear responses, such as chaotic behavior in the postflutter regime.<sup>7</sup> It has also been shown that the presence of a cubic nonlinearity even in a single degree of freedom can give rise to chaotic response for certain specific structural parameters.<sup>8</sup> On the other hand, observations of chaos in aeroelastic response have been reported even in preflutter regimes by the introduction of a freeplay nonlinearity.<sup>4,6,9–11</sup>

The traditional paradigms adopted by the above literature to investigate the aeroelastic problems, by and large, involve an assumption of uniform and nonfluctuating flow. In other words, the flow is assumed to be a deterministic parameter. However, realistic flows in field possess randomly time-varying fluctuations.<sup>12,13</sup> The presence of input flow fluctuations can cause twofold changes: (i) disrupt the traditionally established Hopf bifurcation, by giving rise to atypical preflutter responses<sup>14,15</sup> and (ii) change the stability boundary.<sup>16–18</sup> The present study focuses on the former issue.

Stochasticity in input flows ensures that even at very low values of mean flow speeds, the response (the pitch and the plunge responses) does not fully die down. Furthermore, at intermediate values of mean flow speeds (lower than the critical speed), a

noise induced intermittent aeroelastic response has been reported in the literature.<sup>14,16,19,20</sup> The qualitative nature of intermittent aeroelastic responses has been shown to be dependent on the time scales present in the input fluctuating flow, relative to that of the aeroelastic system.<sup>15</sup> Numerical experiments carried out by Venkatramani *et al.*<sup>18</sup> revealed that based on the intensity of flow fluctuations, the trajectories of the response keep moving between one attractor to another (here, a fixed point response and LCOs) in an unpredictable fashion. Consequently, the concepts of stochastic bifurcations were invoked to describe such a transition from intermittency to flutter.

Through this, it becomes evident that flow fluctuations give rise to atypical flutter routes via intermittency. In the wake of literature investigating flutter (under deterministic flows) using the traditional paradigms of modal frequencies, it is imperative that the mechanism of intermittency route to flutter requires a systematic investigation. The present study focuses on the same. Particularly, we examine the coupled interactions between the pitch and the plunge modes during intermittency route to flutter. The instantaneous interactions between the pitch and plunge modes, in the context of the relative phase, have been discussed in the literature, but they are largely restricted to the unstable flutter regime.<sup>1</sup> The coupling between the pitch and the plunge modes and the presence of a constant phase locking in the flutter regime naturally motivates one to investigate the presence of synchrony in the system, during the transition to flutter. To the best of the authors' knowledge, investigating the evolution of the relative phase difference as the system transitions from the regime of intermittency to flutter has not received any attention in the literature. The same is addressed using the framework of synchronization theory in this study. Using this approach, we show that the onset of aeroelastic flutter is the result of not only the locking of the modal frequencies but also the locking of their instantaneous phases.

This study devotes its attention to study the coupled interactions between the pitch and plunge responses under noisy input flows. To that end, we consider a pitch–plunge airfoil with cubic hardening nonlinearity in the pitch degree of freedom. The fluid forces are modeled using a Wagner function based on unsteady aerodynamical formulation.<sup>1</sup> The flow is assumed to be randomly varying with time. In corroboration with the findings presented in Venkatramani *et al.*,<sup>15</sup> flows with two different time scales of fluctuations are considered as separate cases. The mean flow speed is assumed to be the bifurcation parameter. Using the same, a response analysis is systematically carried out first. The instantaneous phases of the aeroelastic responses (both pitch and plunge) are computed using a Hilbert transform based analytic signal approach. A quantitative measure such as phase locking value that describes the underlying synchrony is utilized next. It is shown that irrespective of the time scales of the fluctuating flows, the onset of flutter instability is via a complete phase locking mechanism of synchronization. The transition to this complete phase synchronization is demonstrated to occur gradually, through an intermediate regime of intermittently phase synchronized responses.

The organization of the rest of the paper is as follows. In Sec. II, a brief overview of synchronization between coupled oscillators is given. Section III provides the mathematical model of the structure and the canonical model used to model the flow fluctuations. We discuss the results in Sec. IV. The salient outcomes that emerge from this study are summarized and presented in Sec. V.

## II. SYNCHRONIZATION OF COUPLED OSCILLATORS: AN OVERVIEW

Synchronization, in simple terms, is the adjustment of the rhythms of coupled oscillators.<sup>21</sup> This phenomenon was discovered by Christian Huygens, while observing the locking of the beats of two oscillating pendulums hung over a wall.<sup>22</sup> The strength and the type of mutual coupling were found to play an important role in the process of synchronization.<sup>23</sup> It is to be noted that synchronization is an inherently nonlinear phenomenon,<sup>23</sup> and both periodic and chaotic oscillators have been found to exhibit synchrony.<sup>23–25</sup> The presence of synchrony has been investigated in diverse fields, such as physical,<sup>26</sup> biological sciences,<sup>27</sup> and engineering systems, such as electric circuits<sup>28,29</sup> and thermoacoustic systems.<sup>30–33</sup> Typically, the presence of synchrony is analyzed by examining the instantaneous phases and the frequency of the oscillations. Oscillators with uncorrelated amplitudes, but, exhibiting perfect locking of their instantaneous phases, i.e., the relative phase is constant, are said to be phase synchronized.<sup>34</sup>

The route to synchronization for mutually coupled oscillators can be explained using mechanisms, such as phase locking and suppression of natural dynamics.<sup>23</sup> Insights into the mechanism of synchronization can be obtained by estimating the frequency content and the time evolution of the instantaneous relative phases between the oscillations. Typically, the instantaneous phases of the oscillations are obtained by adopting the analytic signal approach<sup>35</sup> wherein, the analytic signal,  $\zeta(t)$ , is a complex quantity, whose real part is the original signal,  $z(t)$  and whose imaginary part is its corresponding Hilbert transform (HT) given by

$$z_H(t) = (1/\pi) \text{P.V.} \int_{-\infty}^{\infty} \frac{z(\tau) d\tau}{(t - \tau)}, \quad (1)$$

where P.V. is the Cauchy principal value of the integral. Thus, the analytic signal can be written as

$$\zeta(t) = z(t) + iz_H(t) = A(t)e^{i\phi(t)}, \quad (2)$$

where  $\phi(t)$  represents the instantaneous phase, and,  $A(t)$  is the instantaneous amplitude of the signal. Note that, for an aperiodic signal with broadband power spectrum, the instantaneous phase thus calculated from HT is not properly defined. However, it has been shown in an earlier study that the relative phase between two broadband signals calculated through HT closely matches with that calculated through cross correlation.<sup>36</sup> Hence, ignoring the slight inaccuracy involved in calculating the instantaneous phase for broadband signals, we proceed with HT-based instantaneous phases for the present study.

Complete synchronization is exhibited when the relative phase between the oscillators becomes constant or oscillates about a mean value. On the other hand, a monotonous increase or decrease in the relative phase denotes asynchrony between the oscillators. Further, to demarcate the route to synchronization, the “peaks” or the predominant frequencies of the oscillators are estimated and observed as the control parameter is varied. Relative movement of the frequency peaks of the corresponding oscillators toward a common frequency denotes the phase locking mechanism. Suppression of one of the peaks, while the other peak remains stationary denotes

the suppression of natural dynamics mechanism. The movement between the peaks is negligible in comparison to the phase locking mechanism and the frequency peak of one of the oscillators shrinks and disappears, denoting that the dynamics of one of the oscillators is “suppressed” by the other oscillator.

In some cases, phase synchronization is presaged by a regime of intermittent phase synchronization (IPS), where, regions of synchronized oscillations coexist with regions of unsynchronized oscillations.<sup>32,37</sup> In this study, to quantify the amount of phase synchronization between the responses at different regimes, the phase locking value (PLV) of the responses is estimated. The measure,  $\text{PLV} = N^{-1} |\sum_{j=1}^N \exp(i\Delta\phi_j)|$ , where  $\Delta\phi_j = \phi_{j,\text{plunge}} - \phi_{j,\text{pitch}}$  is the instantaneous phase difference between the plunge and pitch responses at the  $j$ th instant. A perfectly synchronized state gives a PLV of 1, while a completely asynchronous state of oscillations gives a PLV close to 0. The PLV for an intermittent synchronization gives a value between 0 and 1. Having presented the necessary theoretical concepts of synchronization, we turn our attention to the mathematical model studied here.

## III. MATHEMATICAL MODEL

### A. Structural model

This subsection presents a description of the structural model of the aeroelastic system. A three-dimensional wing is modeled as a two degrees of freedom pitch–plunge airfoil by considering its bending and torsion modes, respectively. To facilitate oscillations, the airfoil is attached to translational and rotational springs at its elastic axis; see Fig. 1. This model is well established in the literature to analyze aeroelastic systems<sup>1,13,38,39</sup> and is often referred to as “typical section.” Such a model provides two-pronged advantages. One of the governing equations of motion can be cast into a set of second-order ordinary differential equations and in turn reducing the computational complexities. The second advantage of the model is the presence of a limited number of degrees of freedom (pitch and plunge), which in turn provides an easier glimpse into the synchronization behavior in the respective domains of dynamical states. To incur sustained LCOs in the postflutter regime, a cubic hardening nonlinearity in the pitch degree of freedom is assumed. The governing nondimensional equations of motion for such a “typical section” are

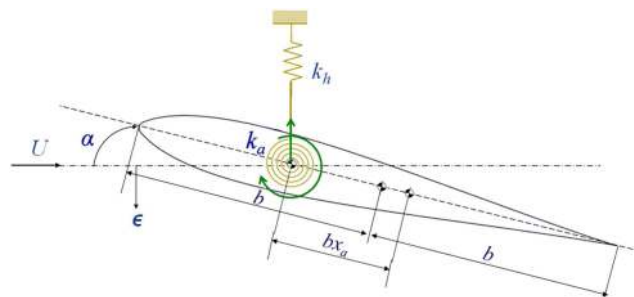


FIG. 1. Schematic of the airfoil section.

TABLE I. Nondimensional parameters of the airfoil.

$r_\alpha$	$\mu$	$x_\alpha$	$a_h$	$\beta_\alpha$	$\zeta_\alpha$	$\zeta_\epsilon$	$\bar{\omega}$
0.5	100	0.25	-0.5	3	0	0	0.2

as follows:<sup>1,39</sup>

$$\epsilon'' + x_\alpha \alpha'' + 2\zeta_\epsilon \frac{\bar{\omega}}{U} \epsilon' + \left(\frac{\bar{\omega}}{U}\right)^2 (\epsilon) = -\frac{1}{\pi\mu} C_L(\tau), \quad (3)$$

$$\frac{x_\alpha}{r_\alpha^2} \epsilon'' + \alpha'' + 2\frac{\zeta_\alpha}{U} \alpha' + \frac{1}{U^2} (\alpha + \beta_\alpha^3) = \frac{2}{\pi\mu r_\alpha^2} C_M(\tau). \quad (4)$$

Here,  $\epsilon$  represents the nondimensional plunge displacement,  $\alpha$  is the pitch displacement expressed in radians,  $\zeta_\epsilon$  and  $\zeta_\alpha$  are the viscous damping ratios in plunge and pitch, respectively,  $\omega_\epsilon$  and  $\omega_\alpha$  are the uncoupled natural frequencies in the plunge and pitch modes, respectively.  $\mu$  is the reduced mass,  $x_\alpha$  is the distance between the elastic axis and the center of mass of the airfoil,  $a_h$  is the distance between the midchord and the elastic axis.  $\bar{\omega}$  is the ratio of plunge to pitch uncoupled natural frequencies,  $\beta_\alpha$  is the coefficient of cubic nonlinear stiffness in pitch,  $r_\alpha^2$  is the radius of gyration, and  $C_L(\tau)$  and  $C_M(\tau)$  are the aerodynamic coefficients which are presented and discussed in Sec. III B. Note that the differentiation is carried out with respect to the nondimensional time  $\tau$ . The structural parameter values used in these equations are taken to be the same as those used in Lee *et al.*<sup>39</sup> and are listed in Table I.

### B. Aerodynamic model

Oncoming flow,  $U$ , results in a displacement of the airfoil, along with the shedding of the wake behind the airfoil’s trailing edge. Therefore, an estimation of the aerodynamic forces demands a relation between the input flow, airfoil displacements, and wake effects. This is achieved by using Wagner’s function<sup>1,40</sup> and in turn invoking an unsteady aerodynamical formulation. The equations are typically cast in the time domain with integrodifferential terms and are mathematically expressed as aerodynamic coefficients given below,

$$C_L(\tau) = 2\pi [\alpha(0) + \epsilon'(0) + (0.5 - a_h)\alpha'(0)]\Phi(\tau) + 2\pi \int_0^\tau \Phi(\tau - \sigma) \times [\alpha'(\sigma) + \epsilon''(\sigma) + (0.5 - a_h)\alpha''(\sigma)]d\sigma + \pi(\epsilon''(\tau) - a_h\alpha''(\tau) + \alpha'(\tau)), \quad (5)$$

$$C_M(\tau) = \pi(0.5 + a_h)[\alpha(0) + (0.5 - a_h)\epsilon'(0) + \epsilon'(0)]\Phi(\tau) + \pi(0.5 + a_h) \int_0^\tau \Phi(\tau - \sigma)[\alpha'(\sigma) + \epsilon''(\sigma) + (0.5 - a_h)\alpha''(\sigma)]d\sigma + \frac{\pi}{2} a_h (\epsilon''(\tau) - a_h\alpha''(\tau) - (0.5 - a_h)\frac{\pi}{2}\alpha'(\tau) - \frac{\pi}{16}\alpha''(\tau)). \quad (6)$$

The time dependent function  $\Phi(\tau)$  in Eqs. (5) and (6) is known as Wagner’s function and is approximated empirically as<sup>1</sup>

$$\Phi(\tau) = 1 - 0.165 \exp(-0.0455\tau) - 0.335 \exp(-0.3\tau). \quad (7)$$

### C. Flow fluctuations

Typical open literature often resorts to using wind spectra, such as Dryden or von Karman spectrum to model the flow fluctuations.<sup>13,17</sup> The flow fluctuations generated through these spectra by and large possess long time scale fluctuations, i.e., the flow fluctuates at a rate much slower than the system scale.<sup>15</sup> A disadvantage of such a spectrum based model is the difficulty in control of the underlying correlation structure. In other words, generation of rapid fluctuations (short time scale fluctuations) becomes computationally tedious. Therefore, in order to gain control of the correlation time of the input flow fluctuations (and in turn the time scales), Venkatramani *et al.*<sup>15</sup> used a canonical model to represent the flow fluctuations.

Accordingly, the flow  $U$  is considered to fluctuate about a mean component  $U_m$  such that,

$$U(\tau) = U_m + f(\tau). \quad (8)$$

Here,  $f(\tau)$  represents the fluctuating component of the flow speed, modeled as a sinusoid with randomly time-varying frequency component as found in Refs. 15, 20, and 41. Thus,  $f(\tau)$  is represented as

$$f(\tau) = \sigma U_m \sin(\omega_r(\tau)\tau). \quad (9)$$

Here,  $\sigma$  represents the intensity of the fluctuations,  $\omega_r(\tau)$  is the frequency of the sinusoid having a random variation with time, such that  $\omega_r(\tau) = \omega_1 + \kappa R(\tau)$ . Note that  $\omega_1$  represents the frequency of the oscillation. This frequency is perturbed by an amount  $\kappa$  at every time step using a uniformly distributed random number generator  $R(\tau)$ . The addition of  $\kappa R(\tau)$  at each time step introduces short time scale fluctuations.

To generate the long time scale fluctuations, one typically resorts to the use of a Karhunen–Loeve Expansion (KLE) as found in Venkatramani *et al.*<sup>15</sup> However, the use of this methodology is rather restricted to isolated cases of extremely long time scales. As the time scales become shorter, one encounters a substantial computational effort in generating the stochastic wind. Further, the use of KLE often demands a Gaussian autocorrelation function. If a non-Gaussian process is involved, one needs to carry out a Nataf’s transformation to obtain the equivalent Gaussian process.<sup>42</sup> This, consequently, leads to further computational difficulties, especially if one needs to vary the scales of the fluctuation. Since the present study anticipates a need for controlling the time scales of the flow fluctuations, a relatively versatile model that alleviates the above issues is considered. By using a moving average filter function, the flow was tailored to fluctuate at a relatively slower rate, thereby generating long time scale fluctuations. A typical moving average function computes the mean of the chosen window and is represented by the following equation:<sup>43</sup>

$$U_n = \frac{\sum_{i=a}^b U_i}{(b - a) + 1}, \quad (10)$$

where  $U_i$  is the flow speed at the  $i$ th instant, limits “a” and “b” are defined by the window size, and  $U_n$  is the average flow speed of the



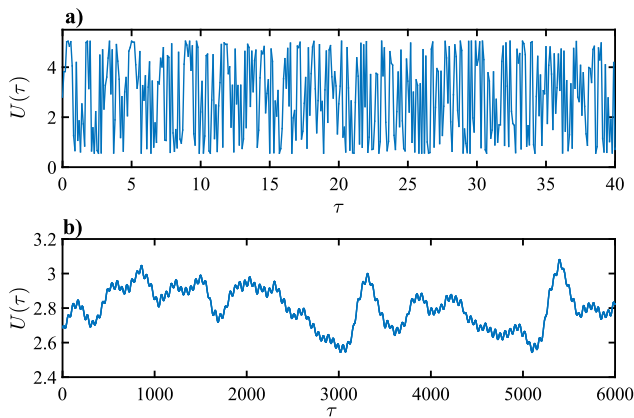


**FIG. 2.** Time variation of the input flow under (a) short time scale fluctuations and (b) long time scale flow fluctuations.

$n$ th window. Changing the window size can generate tailored fluctuations with the requisite correlation time. The “filt” command in MATLAB is used in this study to perform the same.

A sample time history of the short time scale flow fluctuations,  $U(\tau)$ , is shown when  $U_m = 2.8$ ,  $\sigma = 0.8$ ,  $\omega_1 = 0.11$ , and  $\kappa = 0.5$  in Fig. 2(a). The response is shown to vary rapidly with time, indicating the overwhelming presence of very small time scales. This observation is further supported by examining the spectrum of the fluctuations provided in Refs. 15 and 18 and are not repeated here for the sake of brevity. Figure 2(b) shows a sample representation of a long time scale flow fluctuation, where  $U_m = 2.8$ ,  $\sigma = 0.2$ , and a window size of 500 [which is equal to  $(b - a) + 1$  in Eq. (10)] is used in the filter function. The values of  $\omega_1$  and  $\kappa$  remain the same. On visually investigating the response, it becomes evident that the response is quite different from Fig. 2(a). The fluctuation of the flow is relatively very gradual with time. It is worth remembering that here only a qualitative description of the “short” and “long” time scale fluctuations are provided. A rigorous discussion and quantitative analysis of the same can be found in Venkatramani *et al.*<sup>15</sup>

#### IV. RESULTS AND DISCUSSIONS

This section focuses on investigating the coupled interaction between the pitch and the plunge modes as the dynamics transitions to aeroelastic flutter through a state of intermittency. The governing equations of motions [Eqs. (3)–(6)] are solved using an adaptive time step based Runge Kutta algorithm in MATLAB. A stringent tolerance measure for the time step is imposed. With the mean flow speed ( $U_m$ ) as a bifurcation parameter, the aeroelastic responses (pitch and plunge motions) are systematically obtained. First, the route to flutter via intermittency is shown by presenting the time histories of the responses. Next, the presence of synchrony between the pitch and the plunge modes at different dynamical states is identified through qualitative and quantitative measures.

#### A. Intermittency route to aeroelastic flutter

In the absence of flow fluctuations, the aeroelastic response dies down for  $U < U_{cr}$ . Here,  $U_{cr}$  is the critical speed [see Fig. 3(a)-I]. At  $U \geq U_{cr}$ , the responses transform itself into LCOs via a Hopf bifurcation;<sup>44</sup> refer Fig. 3(a). Using the parameters provided in Lee and Leblanc,<sup>44</sup> the onset of flutter is identified to be  $U_{cr} = 6.2$ . However, the physical mechanism behind the dynamics observed in the presence of fluctuating flows deserves a closer look. The transition from a low amplitude responses to LCOs is found to occur through a regime of intermittent oscillations [see Figs. 3(b)-II and 3(c)-II for short and long time scale flow fluctuations, respectively], where segments of periodic oscillations coexists with segments of comparatively lower amplitude aperiodic oscillations. This dynamical state is characterized as intermittency.

In aeroelastic systems, the interplay between the relative time scales of the input flow fluctuations with respect to the natural time scales of the structural modes dictates the qualitative type of intermittency.<sup>45</sup> If the flow possesses predominantly long time scales, then one encounters an “on-off” type intermittency in the preflutter response.<sup>46</sup> The response randomly alternates between large amplitude periodic oscillations, called “on” state, amidst near rest states, called “off” state [see Fig. 3(c)-II]. On the other hand, flows with rapid fluctuations, i.e., with short time scales, give rise to “burst” type intermittency. In this case, the response randomly alternates between “bursts” of periodic oscillations, interspersed amidst aperiodic oscillations [see Fig. 3(b)-II]. In both these cases, as the mean flow speed is increased close to the critical speed, the “bursts” or “on” states appear more frequent with large amplitudes, eventually giving rise to sustained LCOs [see Figs. 3(b)-III and 3(c)-III]. Note that the response dynamics presented here are qualitatively similar to that presented in the wind tunnel experiments by Venkatramani *et al.*<sup>20,41,47</sup>

#### 1. Dynamics under short time scale flow fluctuations

The pitch and plunge responses obtained when the airfoil is subjected to short time scale flow fluctuations are presented in Fig. 4. The noise intensity “ $\sigma$ ” is of the  $\mathcal{O}(1)$ . It is worth mentioning that the purpose of presenting overlapping time series in Fig. 4 is to only showcase the dynamical signature of the system. A noisy low amplitude response is observed at a mean speed  $U_m = 2.8$ , as shown in Fig. 4(a). At a mean speed  $U_m = 5.2$ , the responses comprise of sporadic burst of periodic oscillations amidst relatively low amplitude aperiodic oscillations. This signature is characteristic of “burst” type intermittency and is shown in Fig. 4(b). The bursts of periodic oscillations increase with the mean flow speed  $U_m$  and finally gives rise to fully developed LCOs. The responses exhibiting large amplitude LCOs at  $U_m = 10.5$  are shown in Fig. 4(c). It can be observed that the amplitudes of the plunge responses ( $\epsilon$ ) are observed to vary with time in relative comparison to the pitch responses ( $\alpha$ ). The addition of a cubic hardening nonlinearity in the torsional mode ( $\alpha$ ), perhaps, makes it less susceptible to the fluctuating nature of the flow and explains the seemingly uniform nature of the response amplitude. Additionally, the location of the nonlinear hardening stiffness might explain the relatively lower amplitude of the pitch response ( $\alpha$ ) in comparison to that observed in the plunge response ( $\epsilon$ ). However, one notes that the pitch response has a higher amplitude as shown in Fig. 4(a). An interplay between the noise parameters and the

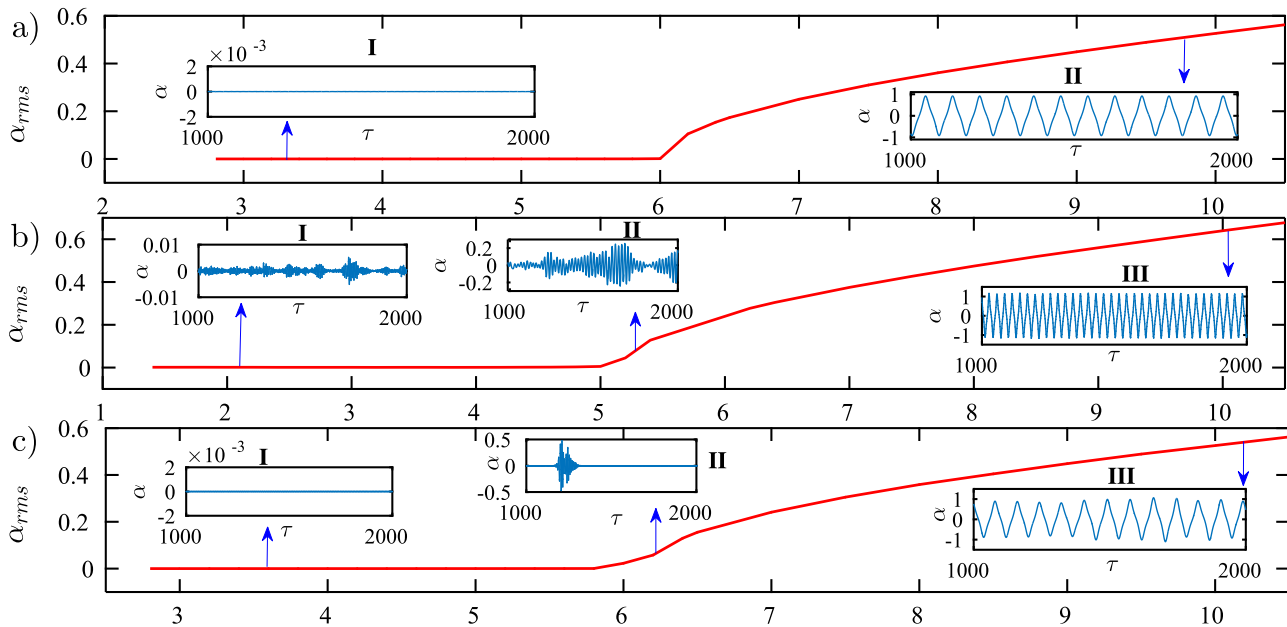


**FIG. 3.** A plot between the root mean square (RMS) of the pitch responses vs mean flow speed in (a) uniform flow conditions (in the absence of fluctuations  $U_m \equiv U$ ), (b) short time scale flow fluctuations, and (c) long time scale flow fluctuations. The responses display a Hopf bifurcation in (a). Any initial disturbance dies down at speeds  $U < U_{cr}$ , and, at speeds higher than  $U_{cr}$ , LCOs are exhibited. The flutter regime is presaged by a regime of intermittent oscillations characterized as “burst” intermittency in (b), and, “on-off” intermittency in (c). It can also be observed that the onset of flutter occurs at speeds  $U_m > 5.2$  in (b) and  $U_m > 6.2$  in (c), owing to the difference in the noise intensities of the flow fluctuations. Similar dynamics are observed in the plunge responses and are not shown here for the sake of brevity.

cubic nonlinearity in the system could perhaps explain this particular response. However, the present study is largely restricted on investigating the presence of synchrony in the pitch and plunge motions during the intermittency route to flutter. Hence, investigating the

interplay between the noise parameters and the nonlinearity of the system requires separate attention, and, is not the main focus of this study.

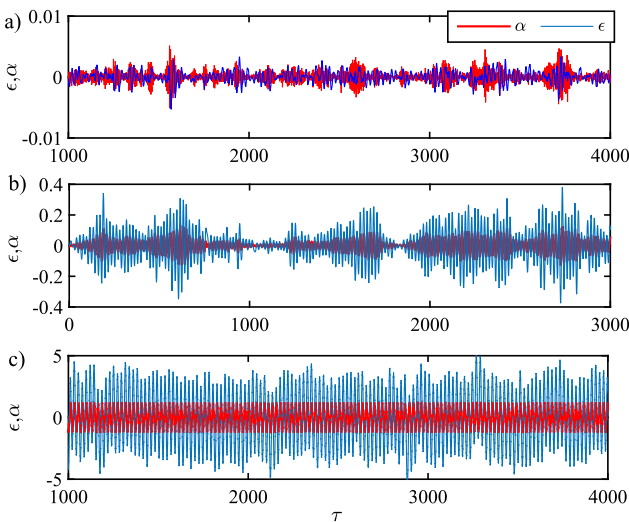


**FIG. 4.** Time histories of the pitch and plunge responses at (a)  $U_m = 2.8$ , (b)  $U_m = 5.2$ , and, (c)  $U_m = 10.5$  generated using short time scale fluctuations.

## 2. Dynamics under long time scale flow fluctuations

The pitch and plunge responses obtained when the airfoil is subjected to predominantly long time scales are shown in Fig. 5. At mean speeds  $U_m < 6.2$ , a damped signature is observed in both the pitch and plunge responses [refer to Fig. 5(a)]. A closer inspection reveals very small amplitude noisy oscillations to exist, owing to the fluctuating input wind. However, since the noisy oscillations possess amplitudes in  $\mathcal{O}(10^{-7})$ , for all intents and purposes, the response characteristics are referred to as damped oscillations. However, the framework of synchronization theory demands the presence of self-sustaining oscillations, and, consequently, the responses obtained at  $U_m < 6.2$  are not taken into this study. Responses exhibiting intermittency at a mean speed  $U_m = 6.2$  are shown in Fig. 5(b). A visual inspection of the time responses shown in Fig. 5(b) suggests that the intermittency is qualitatively different from that shown in Fig. 4(b). Indeed, the response intermittently switches between “on” states of periodic oscillations and “off” states of decaying oscillations resulting in an “on-off” intermittency. Further, upon increasing the mean flow speed, it is observed that the “on” states become more prevalent in terms of amplitude and frequency of occurrence and finally gives rise to LCOs. Responses exhibiting large amplitude LCOs obtained at  $U_m = 10.5$  are shown in Fig. 5(c).

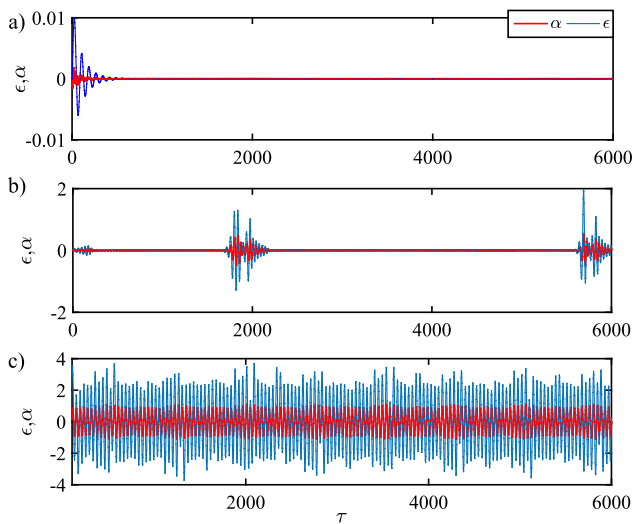


**FIG. 5.** The representative time series of the pitch and plunge responses at (a)  $U_m = 2.8$ , (b)  $U_m = 6.2$ , (c)  $U_m = 10.5$  using long time scale flow fluctuations.

So far, it was shown that in the presence of input flow fluctuations, an intermittency route to flutter exists. Furthermore, based on the scales of flow fluctuations, two different qualitative types of intermittency exist in the preflutter regime. We now turn our attention to investigate the instantaneous interactions between the pitch and the plunge modes during the transition to flutter.

## B. Synchronization of the pitch and plunge oscillations

In this subsection, we proceed to investigate the synchronization characteristics of these responses. To that end, the pitch and plunge degrees of freedom are assumed to be two, coupled, nonidentical oscillators. It is to be noted that the term nonidentical is used to signify the difference in the modal signature of the oscillations (for the present study, the ratio of the uncoupled modal frequencies,  $\bar{\omega}$  is taken as 0.2). First, the frequency content of the pitch and plunge responses is computed by estimating the corresponding Fast Fourier Transform (FFT). Then, the evolution of the relative phase between the responses exhibiting different dynamics is observed, and, the coupled interaction between the modes is explored to demarcate the type of synchrony that is being exhibited.

### 1. Frequency domain analysis

The aeroelastic responses obtained when subjected to short time scale flow fluctuations are analyzed in the frequency domain by computing the corresponding FFTs, and the same along with the variation of their dominant frequencies are shown in Fig. 6. It is well established that under uniform flows aeroelastic flutter manifests when the pitch and the plunge frequencies coalesce at a critical speed. In the present case, distinct frequency peaks can be observed for the low amplitude, noisy response obtained at  $U_m = 2.8$  [see Fig. 6(a)]. The fact that the frequency ratio of these distinct peaks

is close to 0.2 (here this ratio is approximately equal to 0.23) indicates the minimal coupling between the pitch and plunge motion at this flow speed. The responses exhibiting intermittency at a mean speed,  $U_m = 5.2$  [see Fig. 6(b)] appear to have the same frequency peak; however, a broader frequency band in comparison to Fig. 6(c) is observed. The broadband frequency response characterizes the aperiodic segment of the intermittent oscillations, and their corresponding response exhibiting “burst” intermittency is shown in Fig. 4(b). At flow speeds  $U_m \geq 5.2$ , the dominant frequencies of the pitch and plunge responses merge (see Fig. 6), marking the onset of LCOs. Responses exhibiting LCOs, obtained at  $U_m = 10.5$ , display a single frequency peak as shown in Fig. 6(c), and, on comparison with Fig. 6(b) appears to have a narrower bandwidth.

Similarly, the responses obtained using long time scale flow fluctuations at various mean speeds are shown in the frequency domain in Fig. 7. The responses exhibiting “on-off” intermittency at a mean speed  $U_m = 6.2$  display a broadband response with multiple frequency peaks [see Fig. 7(a)]. These peaks give rise to the “on” states present in the response (refer Fig. 5(b)). The responses exhibiting LCOs display a single dominant frequency, as shown in Fig. 7(b). The coalescence of the dominant frequencies of the pitch and plunge responses against the mean flow speed ( $U_m$ ) is shown in Fig. 7 (middle). The modal frequencies are shown to coalesce after a mean speed of  $U_m = 6.2$ , marking the onset of LCOs, and the frequency band is much narrower in comparison to the responses exhibiting intermittency.

### 2. Identification of synchronization states from relative phase dynamics

In the earlier part, the transition to flutter has been discussed in terms of frequency coalescence. Distinct frequencies of the pitch and plunge responses exist at very low flow speeds, and, a single peak with a broader frequency band is present in the preflutter regime. On increasing the flow speed, a single frequency peak with a narrower bandwidth is exhibited at the onset of flutter. The instantaneous interactions between the pitch and the plunge modes are investigated by estimating the instantaneous phases of the signal using the Hilbert transform based analytic signal approach as explained in Sec. II. The evolution of the relative phase ( $\Delta\phi$ ) between the pitch and plunge responses is presented next for different dynamical states corresponding to both short and long time scale fluctuations.

The relative phase between the responses obtained from short time scale fluctuations is shown in Fig. 8. The low amplitude noisy response obtained at  $U_m = 2.8$  [see Fig. 4(a)] has distinct pitch and plunge frequency peaks, as shown in Fig. 6(a). The corresponding relative phase ( $\Delta\phi$ ) is observed to steadily decrease, as shown in Fig. 8(a). This monotonous increase or decrease in the relative phase is termed as “phase drift,” and, it denotes “asynchrony” between the pitch and plunge responses.<sup>33</sup> At a flow speed of  $U_m = 5.2$ , the responses were observed to exhibit “burst” intermittency [refer to Fig. 4(b)], and a broad banded frequency response was also observed [see Fig. 6(b)]. The corresponding phase difference fluctuates about a mean value for a certain period of time, after which it “slips” to a new mean value. In other words, the relative phase is bounded intermittently [refer to Fig. 8(b)]. To further examine the presence of synchronous and asynchronous states, the evolution of the relative



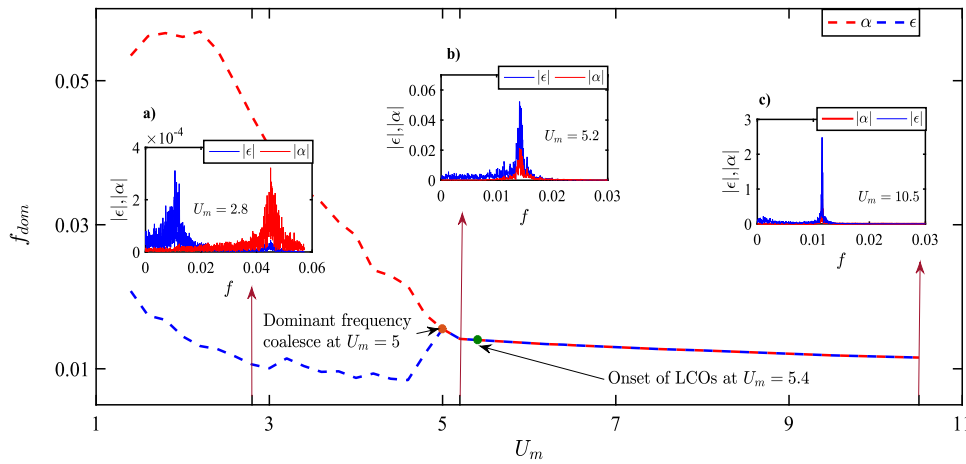


**FIG. 6.** A plot of the dominant frequency ( $f_{dom}$ ) of the pitch and plunge responses against the mean flow speed ( $U_m$ ). The coalescence of the dominant frequencies as the flow speed is increased is shown. Amplitude spectra of the pitch and plunge responses obtained when the structure is subjected to short time scale flow fluctuations at mean flows speeds (a)  $U_m = 2.8$ , (b)  $U_m = 5.2$ , (c)  $U_m = 10.5$ . Distinct frequency peaks are observed for (a) low amplitude aperiodic fluctuations. A broadband frequency response with a single frequency peak is observed for an intermittent response (b). A single frequency peak with a narrower bandwidth is observed for responses exhibiting LCOs in (c).

phase is shown in Fig. 9(a), with the pitch and plunge responses in the inset. The responses in Fig. 9(b) show a synchronous behavior, where the amplitude peaks largely occur at the same time, and the relative phase fluctuates about a constant. However, in Fig. 9(c), the

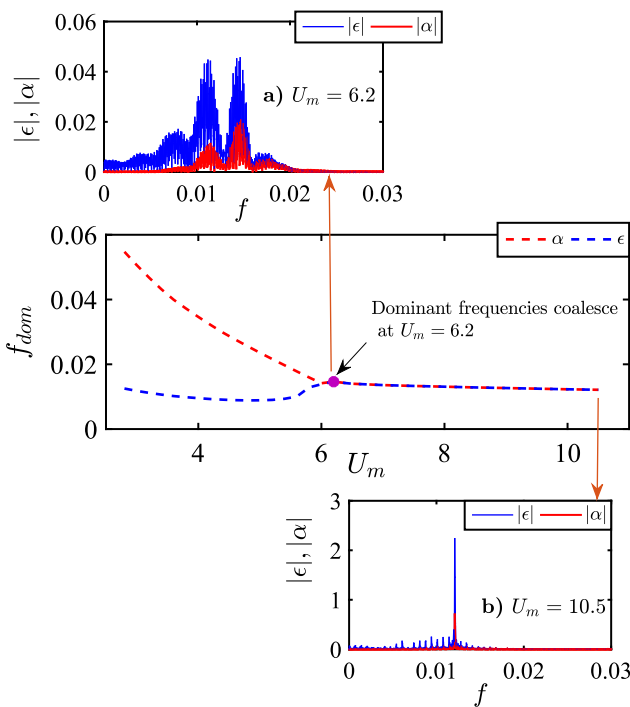


**FIG. 7.** A plot of the dominant frequencies ( $f_{dom}$ ) of the pitch and plunge responses vs mean flow speed ( $U_m$ ). The coalescence of the dominant frequencies as the flow speed is increased is shown (middle). Amplitude spectra of the pitch and plunge responses obtained when the structure is subjected to long time scale flow fluctuations at mean flows speeds (a)  $U_m = 6.2$ , (b)  $U_m = 10.5$ . A broadband frequency response with multiple frequency peaks is observed for an intermittent response shown in (a). A single frequency peak with a narrower bandwidth is observed for responses exhibiting LCOs in (b).

amplitude of the aperiodic responses is relatively small and shows no correlation with each other, thus it can be classified as an asynchronous behavior, leading to the phase slip.<sup>32</sup> The stage at which the relative phase oscillates about a mean value denotes synchronization of the responses. The slip denotes imperfection in the phase locking of the responses, due to a phase jump in any one of the responses (here the pitch response). This coexistence of synchronous

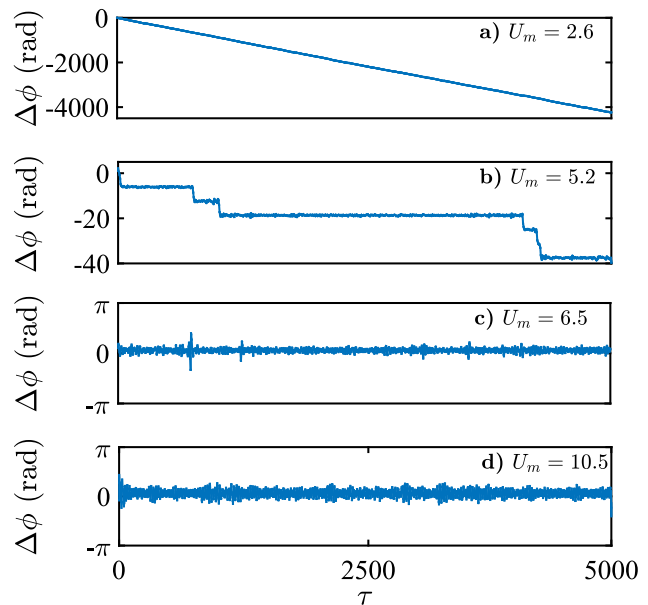


**FIG. 8.** The relative phase between the pitch and plunge responses obtained from short time scale flow fluctuations at mean speeds (a)  $U_m = 2.8$ , (b)  $U_m = 5.2$ , (c)  $U_m = 6.5$ , (d)  $U_m = 10.5$ . A steady decrease in relative phase difference is observed in (a). The phase difference oscillates about a mean value for some time period and then decreases to a new mean value in (b). Phase slips occur in the integer multiple of  $2\pi$  in between two consecutive synchronization regions. The phase difference oscillates about a mean value in (c) and (d), denoting synchrony.

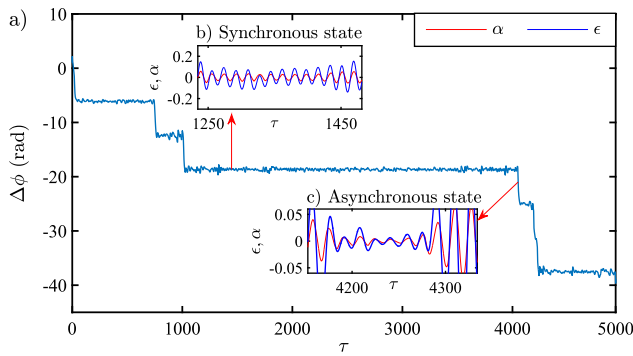


**FIG. 9.** (a) The evolution of the relative phase between the pitch and plunge responses during intermittency. The pitch and plunge responses are shown in the insets when (b) the phase difference fluctuates about a constant, and, (c) the phase difference slips. The bursts of periodic responses was found to exhibit a synchronous behavior, as shown in (b). The relatively low amplitude aperiodic response was found to exhibit an asynchronous response, which corresponds to the phase slip, as shown in (c).

and asynchronous states is referred to as intermittent phase synchronization (IPS).<sup>32</sup> The phase difference of the responses at a mean flow speed of  $U_m = 6.5$  and  $10.5$  as shown in Figs. 8(c) and 8(d) oscillates about a mean value of zero. It is also to be noted that the responses exhibit LCOs at this mean speed. The bounded oscillations of the relative phase denote synchrony between the pitch and plunge responses. We now turn our attention to the synchronization behavior between pitch and plunge responses when long time scale fluctuations are used.

The evolution of the relative phase between the responses obtained from long time scale flow fluctuations is shown in Fig. 10. As mentioned earlier, responses at speeds lower than  $U_m < 6.2$  have been neglected. In Fig. 10(a), the phase difference exhibiting IPS is shown. The evolution of the corresponding pitch and plunge response time histories is shown in the inset of Fig. 10(a). In the vicinity of  $\tau = 6000$ , the phase difference was found to initially decrease. On closer inspection, the responses were found to exhibit an “on” state in the same time interval. It can be observed that the amplitude peaks of the pitch and plunge responses remain largely uncorrelated at the beginning of the “on” state, thus the decreasing phase difference denotes asynchrony. However, toward the end of the “on” state, the amplitude peaks occur at the same time, indicating a constant phase difference which remains constant even at the “off” state, where the small amplitude oscillations exist in a synchronous state. As discussed earlier, this denotes the intermittent phase synchronization of the responses. The phase difference is observed to oscillate about a mean value at  $U_m = 10.5$  [see Fig. 10(b)], denoting synchronization between the pitch and plunge responses.

Hence, it can be summarized that the transition to flutter is through a regime of intermittent phase synchronization of the pitch and plunge modes, and, at the onset of flutter, the pitch and the plunge modes exist in a state of complete synchronization. Having looked into the synchronization transition qualitatively, we now investigate the presence of synchrony quantitatively by estimating the PLV at

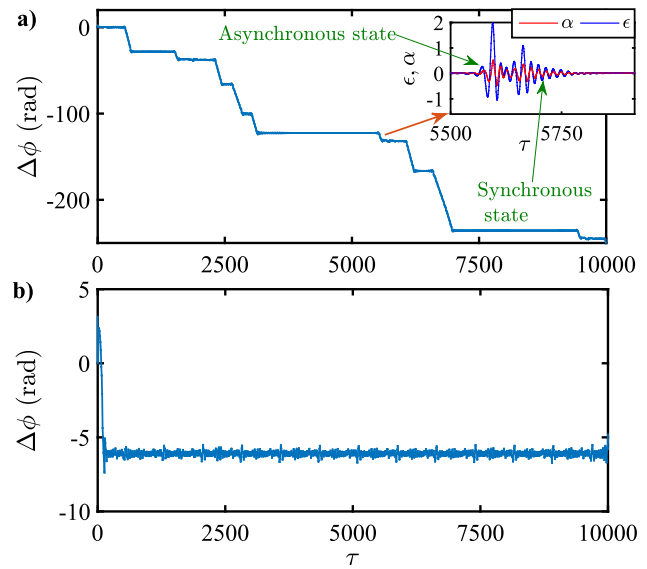


**FIG. 10.** The relative phase between the pitch and plunge responses obtained from long time scale flow fluctuations at mean speeds (a)  $U_m = 6.2$ , (b)  $U_m = 10.5$ . The alternating nature of the phase difference observed, exhibits a staircase like response in (a), corresponding to intermittent phase synchronization of the responses. The same is explained with the help of the corresponding pitch and plunge responses at  $\tau = 6000$  provided in the inset in (a). The phase difference fluctuates about a mean value in (b) denoting synchronization between the pitch and plunge responses.

different dynamics for both short time scale and long time scale flow fluctuations.

A plot between the PLV and the mean flow speed ( $U_m$ ) of the responses obtained from flow speeds with short time scale fluctuations is shown in Fig. 11. In region 1, the PLV remains lower than unity and is observed to increase with the mean flow speed. This region corresponds to the preflutter regime, consisting of very low amplitude noisy responses and intermittent oscillations, existing as a combination of periodic and aperiodic oscillations. As the flow speed is increased, the aperiodic bursts reduce and sustained large amplitude periodic oscillations begin to manifest. This increases the PLV value signifying that the periodic oscillations correspond to “synchronous” states and the relatively lower amplitude aperiodic oscillations correspond to “asynchronous” states. The manifestation of limit cycle oscillations in region 2 further substantiates this claim, as the PLV remains very close to 1. FFTs of the pitch and plunge responses given in the inset [see Figs. 11(b)–11(d)] show the coalescence of the frequency peaks as the mean flow speed increases. Also, the relative movement of both the peaks emphasizes that, here, the phase locking mechanism paves the way to synchronization. The evolution of the relative phase is shown in Figs. 11(e)–11(g). The phase difference shown in Fig. 11(f) denotes intermittent phase synchronization, and in Fig. 11(g), complete phase synchronization is displayed.

Next, the PLV of the responses obtained when the structure is subjected to long time scale fluctuations is presented in Fig. 12. In

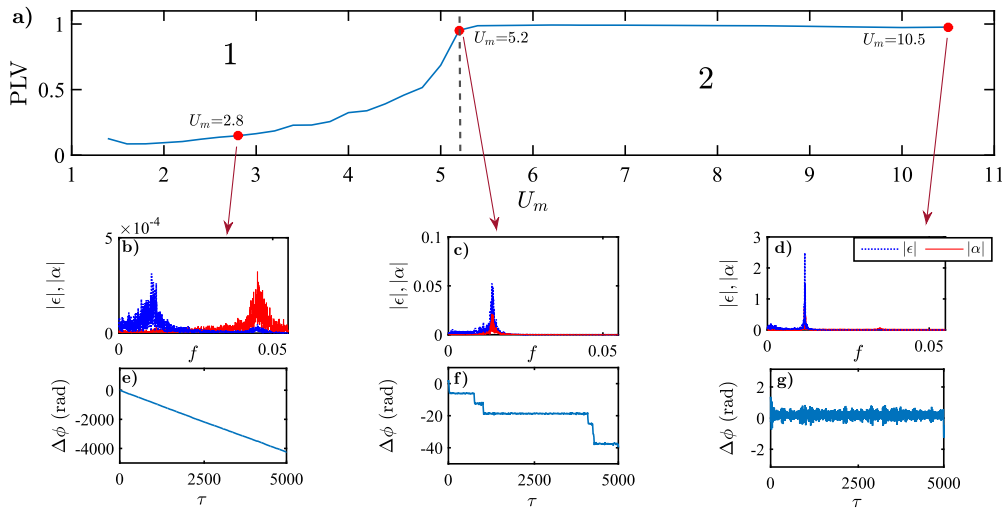


**FIG. 11.** (a) A plot of PLV vs  $U_m$  obtained for short time scale fluctuations. The red markers indicate the points on the plot at  $U_m = 2.8, 5.2,$  and  $10.5$ . Amplitude spectra of the pitch and plunge responses are presented in the inset at speeds (b)  $U_m = 2.8,$  (c)  $U_m = 4.2$  and (d)  $U_m = 10.5$ . The corresponding evolution of the relative phase difference are shown in (e)–(g).

region 1, the PLV value is lesser than 1 and is found to increase with the mean flow speed  $U_m$ . At a mean speed  $U_m = 6.2$ , the responses exhibit intermittent phase synchronization [refer to Fig. 12(d)], explaining the low PLV value. On further increasing the mean speed, the “on” states become more prevalent, both in amplitude and frequency of occurrence, thus explaining the increase in PLV value. In region 2, the responses exhibit large amplitude LCOs that largely remain in a synchronous state [refer to Fig. 12(e)].

From Figs. 11 and 12, the responses evolve from a state of asynchrony (shown only for short time scale fluctuations) to phase synchronization through a period of intermittent phase synchronization, regardless of the time scale of the flow fluctuations that the airfoil was being subjected to. Since phase synchronization was found only in the regime of LCOs, it can be understood that the synchronization of the pitch and plunge responses leads to the dynamic instability, and, its gradual transition is through a

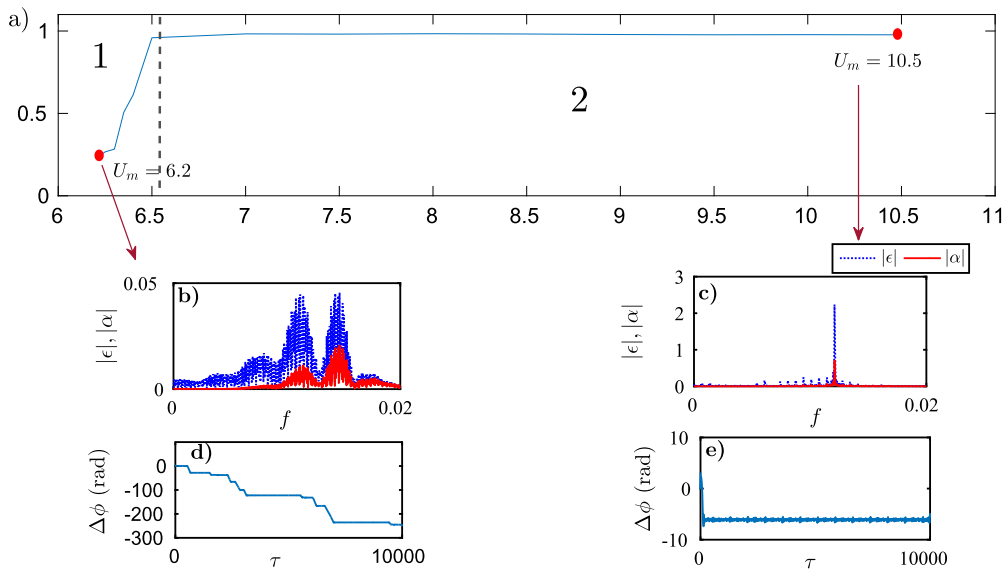


**FIG. 12.** (a) A plot of PLV vs  $U_m$  obtained for long time scale flow fluctuations. The red markers indicate the points on the plot at  $U_m = 6.2$  and  $10.5$ . Amplitude spectra of the pitch and plunge responses are presented in the inset at speeds (b)  $U_m = 6.2$  and (c)  $U_m = 10.5$ . The corresponding evolution of the relative phase difference are shown in (d) and (e).

regime of intermittent phase synchronization of the pitch and plunge responses.

## V. CONCLUDING REMARKS

This study dealt with investigating coupled interactions between the pitch and the plunge modes for an aeroelastic system under fluctuating flows. A pitch–plunge airfoil was investigated under fluctuating flows and the observed dynamics were discussed under the purview of synchronization. The mutual synchronization of the pitch and plunge responses was shown as a possible mechanism for intermittency route to flutter. The presence of synchrony was identified by investigating the evolution of the relative phase between the pitch and the plunge modes and by computing the PLV at different mean flow speeds. It was found that a mixture of synchronous and asynchronous states existed in the preflutter regime, i.e., during intermittency. At the onset of flutter, the responses were observed to show complete phase synchronization. The above observations were exhibited irrespective of the scales present in the input fluctuating flow.

Though the present study is the first of its kind to invoke the concepts of synchronization theory to describe the intermittency route to flutter, a number of other features could be considered to strengthen the findings. For instance, examining our findings in light of other nonlinearities is necessary. This in turn would involve ascertaining the bifurcation and response characteristics as a first step before examining the system under the framework of synchronization. Similarly, the role of noise intensity in affecting the extent of synchrony was not explored. Studies in the literature,<sup>16,18</sup> however, present that the intensity of noise can substantially alter the dynamics, which in turn can influence the amount of phase synchronization. Further, the interplay between noise intensity and the underlying time scales can affect the laminarity length of intermittent responses.<sup>46,47</sup> Therefore, a symbiotic change in scales and fluctuation intensity possesses the potential to alter the synchronization description presented here. The authors believe that a systematic stochastic bifurcation study must be employed to quantify the above and are interesting problems to be taken up next.

## REFERENCES

- Y. Fung, *An Introduction to the Theory of Aeroelasticity* (Wiley, New York, 1955).
- D. H. Hodges and G. A. Pierce, *Introduction to Structural Dynamics and Aeroelasticity* (Cambridge University Press, 2011), Vol. 15.
- S. Cole, in *31st Structures, Structural Dynamics and Materials Conference*, NASA Technical Memorandum 102622, 1990, p. 981.
- H. Alighanbari, “Flutter analysis and chaotic response of an airfoil accounting for structural nonlinearities,” Ph.D. thesis (McGill University Libraries, 1995).
- T. O’Neil and T. W. Strganac, *J. Aircr.* **35**, 616 (1998).
- B. Lee, L. Jiang, and Y. Wong, *J. Fluids Struct.* **13**, 75 (1999).
- B. H. Lee and L. Liu, *J. Aircr.* **43**, 652 (2006).
- L. Daochun and X. Jinwu, *J. Aircr.* **45**, 1457 (2008).
- A. Hauenstein, R. Laurenson, W. Everman, G. Galecki, and A. Amos, in *31st Structures, Structural Dynamics and Materials Conference* (AIAA, 1992), p. 1034.
- L. Virgin, E. Dowell, and M. Conner, *Int. J. Non Linear Mech.* **34**, 499 (1999).
- L. Liu, Y. Wong, and B. Lee, *J. Sound Vib.* **253**, 447 (2002).
- F. M. Hoblit, *Gust Loads on Aircraft: Concepts and Applications* (American Institute of Aeronautics and Astronautics, 1988).
- D. Poirel and S. Price, *J. Fluids Struct.* **18**, 23 (2003).
- B. Korbahti, E. Kagambage, T. Andrianne, N. A. Razak, and G. Dimitriadis, *J. Fluids Struct.* **27**, 408 (2011).
- J. Venkatramani, S. Krishna Kumar, S. Sarkar, and S. Gupta, *J. Fluids Struct.* **75**, 9 (2017).
- D. C. M. Poirel, “Random dynamics of a structurally nonlinear airfoil in turbulent flow,” Ph.D. dissertation (McGill University, 2001).
- D. Zhao, Q. Zhang, and Y. Tan, *Nonlinear Dyn.* **58**, 643 (2009).
- J. Venkatramani, S. Sarkar, and S. Gupta, *Nonlinear Dyn.* **92**, 1225 (2018).
- T. Andrianne and G. Dimitriadis, in *Proceedings of the 8th International Conference on Structural Dynamics, EURO-DYN 2011* (Katholieke Universiteit Leuven, 2011), pp. 1341–1347.
- J. Venkatramani, V. Nair, R. Sujith, S. Gupta, and S. Sarkar, *J. Fluids Struct.* **61**, 376 (2016).
- A. Pikovsky, M. Rosenblum, and J. Kurths, *Synchronization: A Universal Concept in Nonlinear Sciences* (Cambridge University Press, 2003), Vol. 12.
- M. G. Rosenblum, A. S. Pikovsky, and J. Kurths, *Phys. Rev. Lett.* **76**, 1804 (1996).
- A. Balanov, N. Janson, D. Postnov, and O. Sosnovtseva, *Synchronization: From Simple to Complex* (Springer Science & Business Media, 2008).
- I. Blekhan, P. S. Landa, and M. G. Rosenblum, *Appl. Mech. Rev.* **48**, 733 (1995).
- S. Boccaletti, J. Kurths, G. Osipov, D. Valladares, and C. Zhou, *Phys. Rep.* **366**, 1 (2002).
- M. Rosenblum and A. Pikovsky, *Contemp. Phys.* **44**, 401 (2003).
- F. Mormann, K. Lehnertz, P. David, and C. E. Elger, *Physica D* **144**, 358 (2000).
- J. F. Heagy, T. L. Carroll, and L. M. Pecora, *Phys. Rev. E* **50**, 1874 (1994).
- R. Roy and K. S. Thornburg, Jr., *Phys. Rev. Lett.* **72**, 2009 (1994).
- S. A. Pawar, S. Mondal, N. B. George, and R. Sujith, *AIAA J.* **57**, 836 (2018).
- S. Mondal, S. A. Pawar, and R. Sujith, in *Energy for Propulsion* (Springer, 2018), pp. 125–150.
- S. A. Pawar, A. Seshadri, V. R. Unni, and R. I. Sujith, *J. Fluid Mech.* **827**, 664693 (2017).
- S. Mondal, S. A. Pawar, and R. I. Sujith, *Chaos* **27**, 103119 (2017).
- M. G. Rosenblum, A. S. Pikovsky, and J. Kurths, *Phys. Rev. Lett.* **78**, 4193 (1997).
- P. F. Panter, *Modulation, Noise, and Spectral Analysis: Applied to Information Transmission* (McGraw-Hill, New York, 1965).
- S. Mondal, V. R. Unni, and R. I. Sujith, *J. Fluid Mech.* **811**, 659681 (2017).
- S. Ahn, C. Park, and L. L. Rubchinsky, *Phys. Rev. E* **84**, 016201 (2011).
- H. Alighanbari and S. J. Price, *Nonlinear Dyn.* **10**, 381 (1996).
- B. Lee, L. Jiang, and Y. Wong, *J. Fluids Struct.* **13**, 75 (1999).
- W. P. Jones, *Summary of Formulae and Notations Used in Two-Dimensional Derivative Theory* (Aeronautical Research Committee, 1942).
- J. Venkatramani, V. Nair, R. Sujith, S. Gupta, and S. Sarkar, *J. Sound Vib.* **386**, 390 (2017).
- M. Aswathy and S. Sarkar, *Int. J. Mech. Sci.* **153–154**, 103 (2019).
- A. V. Oppenheim, J. R. Buck, and R. W. Schaffer, *Discrete-Time Signal Processing* (Prentice Hall, Upper Saddle River, NJ, 2001), Vol. 2.
- B. Lee and P. Leblanc, “Flutter analysis of a two-dimensional airfoil with cubic non-linear restoring force,” Aeronautical Note NAE-AN-36 National Research Council Canada, 1986.
- R. C. Hilborn *et al.*, *Chaos and Nonlinear Dynamics: An Introduction for Scientists and Engineers* (Oxford University Press, 2000).
- N. Platt, E. A. Spiegel, and C. Tresser, *Phys. Rev. Lett.* **70**, 279 (1993).
- J. Venkatramani, S. Sarkar, and S. Gupta, *J. Sound Vib.* **419**, 318 (2018).